J. Fluid Mech. (2019), *vol.* 860, *pp.* 408–418.
doi:10.1017/jfm.2018.885

On the dynamics of a free surface of an ideal fluid in a bounded domain in the presence of surface tension

Sergey A. Dyachenko†

Department of Mathematics, University of Illinois at Urbana-Champaign, Urbana, IL 61801, USA

(Received 18 April 2018; revised 21 October 2018; accepted 26 October 2018;
first published online 7 December 2018)

We derive a set of equations in conformal variables that describe a potential flow of an ideal two-dimensional inviscid fluid with free surface in a bounded domain. This formulation is free of numerical instabilities present in the equations for the surface elevation and potential derived in Dyachenko *et al.* (*Plasma Phys. Rep.* vol. 22 (10), 1996, pp. 829–840) with some restrictions on analyticity relieved, which allows to treat a finite volume of fluid enclosed by a free-moving boundary. We illustrate with a comparison of numerical simulations of the Dirichlet ellipse, an exact solution for a zero surface tension fluid. We demonstrate how the oscillations of the free surface of a unit disc droplet may lead to breaking of one droplet into two when surface tension is present.

Key words: capillary flows, interfacial flows (free surface), waves/free-surface flows

1. Introduction

The motion of the fluid in the ocean is incredibly rich, and numerous phenomena remain unexplained from the theoretical point of view. It is quite common to study water waves on the surface of the ocean, and it is sometimes convenient to introduce conformal variables whose essence is in the mapping of physical fluid to a simpler conformal domain such as the unit circle (Tanveer 1993) or the lower complex plane (Zakharov 1968). The dynamics of the free surface is recovered from a set of equations of motion for the time-dependent conformal map. Introduction of the complex variables suggests a description of dynamics of an irrotational two-dimensional fluid in terms of the dynamics of its complex singularities, yet this theory is still in its infancy.

The first classical results for the motion of the free surface over an ideal two-dimensional fluid have been obtained by Stokes (1880) (the travelling waves), and, before that, a class of exact time-dependent solutions was found by Dirichlet (1860). A detailed study of Dirichlet solutions including the ellipse and the hyperbola was performed by Longuet-Higgins (1972). In the second half of the twentieth century Zakharov (1968) discovered that the surface elevation and the velocity potential on the free surface are canonical Hamiltonian variables. The conformal mapping approach

† Email address for correspondence: sdyachen@math.uiuc.edu

for the Euler description of the full, non-stationary problem was first introduced by Tanveer (1993). In 1996, Dyachenko *et al.* (1996*a*) and Dyachenko, Zakharov & Kuznetsov (1996*b*) established a formulation for non-stationary water waves based on a conformal mapping of the fluid domain. This formulation has proven quite successful for numerical simulations in conjunction with the pseudospectral method. Although these equations have been shown to suffer from numerical instability owing to truncation of the Fourier series, subsequent work by Dyachenko (2001) discovered a reformulation that is free of numerical instabilities and contains only polynomial nonlinearities in the equation. A sequence of works followed in which their numerical simulations were based on this formulation, see, e.g., Zakharov, Dyachenko & Vasilyev (2002). In the following years, various extensions have been developed such as free surface over an undulating bottom (Ruban 2004), and Turitsyn, Lai & Zhang (2009) developed an extension to handle an air bubble encircled by the fluid.

One spectacular nonlinear phenomenon that occurs in the ocean and still defies attempts to fully theoretically explain is the breaking of ocean waves, leading to the formation of air–water foam at the wave crest. The air–water foam, or a whitecap, is a mixture of water droplets and bubbles of air trapped at the surface layer of sea water. The details of the dynamics of the breakers and the water droplets is quite complicated. One of the conjectures that explain formation of whitecaps requires presence of the surface tension force. A numerical demonstration of how this event may occur is illustrated in Dyachenko & Newell (2016). We would like to advance the result of the latter work, and illustrate how the dynamics of a single fluid droplet in a whitecapping event may fracture in a spray of smaller droplets.

In this paper, we derive a mathematical model suited for capturing the motion of an ideal two-dimensional fluid in a bounded domain in the flavour of the equations derived in Dyachenko (2001). Our formulation is capable of approaching the time of the splitting of a droplet, yet we emphasize that we do neglect all the 3D effects in our discussion. We demonstrate our numerical findings, yet we intend to focus on the theoretical aspects of the droplet splitting in subsequent works.

It is common to study water waves on a shear flow assuming constant vorticity throughout the entire fluid volume because of tractability of this formulation, yet when we consider a fluid of infinite depth the assumption of constant vorticity leads to divergence of the velocity of the shear flow away from the free surface. The present formulation describes a fluid whose domain is bounded and, thus, a constant vorticity does not lead to diverging kinetic energy of the fluid. We intend to derive a model that combines a constant vorticity flow in the flavour of Constantin, Strauss & Vărvărucă (2016) and Dyachenko & Mikyoung Hur (2018) and the numerical works of Da Silva & Peregrine (1988) and Ribeiro, Milewski & Nachbin (2017) together with the bounded fluid domain in a subsequent work. An interesting subject can be the study of periodic travelling waves on the boundary of a unit disc in the presence of surface tension similar to the analogous problem in an infinite volume of fluid and its exact solution first discovered by Crapper (1957).

We demonstrate in a simple example how a Dirichlet ellipse (Longuet-Higgins 1972) solution is recovered in a direct numerical simulation when surface tension is absent. However, when an identical initial condition is evolved subject to a surface tension force, the shape of the fluid domain indicates that breaking of a droplet is imminent given that it carries enough kinetic energy. This simulation suggests a possible scenario for how a spray of fluid droplets is produced by surface tension forces. We would like to emphasize that this is a conjecture that is supported by a numerical experiment and is not a theoretical result.

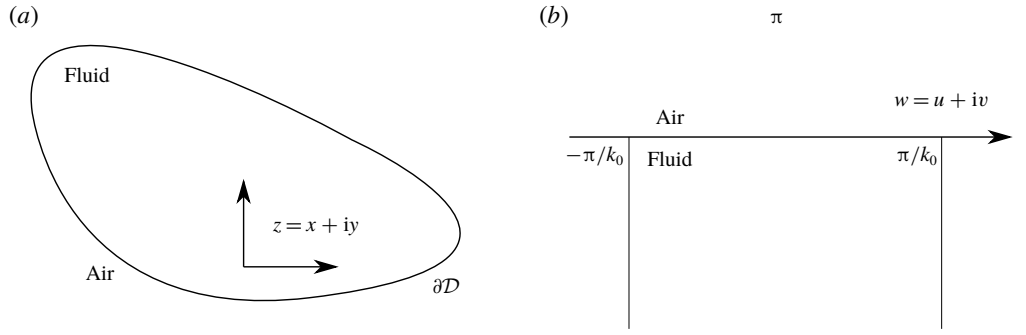

FIGURE 1. Illustration of the conformal map: the fluid domain $z = x + \mathrm{i}y$ is enclosed by the free surface $\partial\mathcal{D}$ (*a*), and the conformal domain $w = u + \mathrm{i}v$ is the periodic strip in the lower complex half-plane (*b*).

2. Formulation of the problem

We study a two-dimensional incompressible fluid that fills a bounded domain $\mathcal{D}$ with mass density $\rho = 1$. The boundary of the fluid domain, $\partial\mathcal{D}(t)$, is a free surface given in the implicit form $F(x, y, t) = 0$. The fluid flow is potential and the velocity field is given by $\boldsymbol{v}(x, y, t) = \nabla\varphi(x, y, t)$ and

$$\nabla^2\varphi = 0. \tag{2.1}$$

The non-stationary Bernoulli equation governs the evolution of the velocity potential, in particular, at $\partial\mathcal{D}$,

$$(\varphi_t + \tfrac{1}{2}(\nabla\varphi)^2 + p)|_{F(x,y,t)=0} = 0, \tag{2.2}$$

where $p = p(x, y, t)$ is the pressure, and the Bernoulli constant was absorbed in φ_t. We neglect the atmospheric pressure at the free surface and have $p = \sigma\kappa$, where σ is the surface tension coefficient and κ is the magnitude of the local curvature.

In general, a fluid particle on the free surface moves in both the tangential and the normal direction; however, it is only the motion in the normal direction that changes the shape of the fluid boundary. This motion is captured by the kinematic boundary condition

$$\frac{\partial F}{\partial t} + |\nabla F|(\nabla\varphi, \boldsymbol{n})|_{F(x,y,t)} = 0, \tag{2.3}$$

where $\boldsymbol{n} = \boldsymbol{n}(x, y, t)$ is the outward unit normal to $\partial\mathcal{D}$ at the point (x, y).

The total energy, $\mathcal{H}$, associated with the fluid flow is given by the sum of the kinetic energy, T, and the potential energy, $\mathcal{U}$:

$$T = \frac{1}{2}\iint_{\mathcal{D}} (\nabla\varphi)^2 \,\mathrm{d}x\,\mathrm{d}y, \quad \mathcal{U} = \sigma\int_{\partial D} \mathrm{d}l. \tag{2.4a,b}$$

Here σ is the coefficient of surface tension and $\mathrm{d}l$ is the elementary arclength along $\partial\mathcal{D}$.

3. Conformal variables

Let $z(w) = x(w) + \mathrm{i}y(w)$ be a conformal map to the fluid domain $(x, y) \in \mathcal{D}$ from a periodic strip $w = u + \mathrm{i}v$, $-\pi \leqslant k_0 u < \pi$, $v \leqslant 0$ and k_0 is the base wavenumber for the parameterization of the circle. The illustration of the mapping is given in figure 1.

The free surface $\partial\mathcal{D}$ is mapped from $v=0$ and satisfies

$$F(x(u,t),y(u,t),t)=0. \tag{3.1}$$

The kinematic condition can be revealed from the observation of the time derivative of the implicit function F, i.e.

$$\frac{\mathrm{d}F}{\mathrm{d}t}=F_t+F_x x_t+F_y y_t=0, \tag{3.2}$$

where the subscript denotes a partial derivative. After a change of coordinates from the (x,y)-plane to the (u,v)-plane, and applying the chain rule it becomes

$$F_t+\frac{x_t x_u+y_t y_u}{|z_u|^2}F_u+\frac{x_t y_u-y_t x_u}{|z_u|^2}F_v=0, \tag{3.3}$$

and the coefficient at F_v gives the rate of change of the free surface $\partial\mathcal{D}$ in the vertical direction in the w-plane, which translates to the normal direction in the (x,y)-plane. In conformal variables (2.3) can be written by noting that the unit normal $\boldsymbol{n}$ is given by

$$\boldsymbol{n}=\frac{1}{|z_u|}(-y_u,x_u)^T, \tag{3.4}$$

where we exploit the fact that $z(w)$ is subject to Cauchy–Riemann (CR) relations. A change of variables in (2.3) thus reveals that

$$F_t+\frac{\psi_v}{|z_u|^2}F_v=0, \tag{3.5}$$

where we have introduced a restriction of the velocity potential to the free surface:

$$\psi(u,t)=\varphi(x,y,t)|_{F(x,y,t)=0}. \tag{3.6}$$

By matching the coefficient at the partial derivative F_v in (3.3) and (3.5), we discover the kinematic condition in the conformal domain,

$$\frac{x_t y_u-y_t x_u}{|z_u|^2}=\frac{\psi_v}{|z_u|^2}, \tag{3.7}$$

which ensures that the line $v=0$ maps to the free surface for all time. Having a derivative with respect to v is a nuisance that can be alleviated by making use of the stream function, θ, and using CR relations together with Titchmarsh's theorem (Titchmarsh 1986) to find that $\psi_v=-\hat{H}\psi_u$, where $\hat{H}$ denotes the Hilbert transform,

$$\hat{H}f(u)=v.p.\int_{-\infty}^{\infty}\frac{f(u')\,\mathrm{d}u'}{u'-u}, \tag{3.8}$$

where $v.p.$ denotes a Cauchy principal value integral.

The Bernoulli equation (2.2) determines the evolution of the velocity potential at the free surface. It is formulated in conformal variables by means of elementary calculus. The force of surface tension is proportional to the local curvature of $\partial\mathcal{D}$:

$$p=-\sigma\frac{x_u y_{uu}-y_u x_{uu}}{|z_u|^3}. \tag{3.9}$$

Under the conformal change of variables the surface potential $\psi(u,t)$ becomes a composite function,

$$\psi(u,t)=\varphi(x(u,t),y(u,t),t), \tag{3.10}$$

the time derivative of which together with (2.2), (3.7) and (3.9) reveal that

$$\psi_t = -\frac{\psi_u^2 - (\hat{H}\psi_u)^2}{2|z_u|^2} + \psi_u \hat{H}\left[\frac{\hat{H}\psi_u}{|z_u|^2}\right] - p, \tag{3.11}$$

the dynamic boundary condition in the conformal domain.

4. The complex equations

In order to reveal the analytic structure of the problem at hand, it is convenient to introduce the complex potential $\Phi = \psi + \mathrm{i}\theta$. By the Titchmarsh theorem, the complex potential can also be written in the form

$$\Phi = \psi + \mathrm{i}\hat{H}\psi = 2\hat{P}\psi, \tag{4.1}$$

where $2\hat{P} = 1 + \mathrm{i}\hat{H}$ and $\hat{P}$ is the projection operator. Both the complex functions Φ and z are analytic in the periodic strip in the lower complex half-plane. Unlike the problem of travelling waves on a fluid of finite or infinite depth, in our formulation the free surface ∂D is a closed curve in the (x, y)-plane and, hence, the conformal map $z(u + \mathrm{i}v)$ must be a periodic function of the variable u, rather than an identity transformation plus a periodic correction. Therefore, $z(w)$ (as well as $\Phi(w)$) is expanded as a Fourier series, and the analyticity in the periodic strip requires that only the non-positive Fourier coefficients are non-zero, i.e.

$$z(w) = \hat{z}_0 + \sum_{k_0\mathbb{N}} \hat{z}_k \mathrm{e}^{-\mathrm{i}kw}, \tag{4.2}$$

where $\hat{z}_k$ denotes the Fourier coefficients of z. As evident from this expansion, as $w \to -\mathrm{i}\infty$ the derivative of the conformal map $z_w \to 0$ and $z(w \to -\mathrm{i}\infty) = z_0$. In other words, we define a new analytic function $\rho(w)$ that satisfies

$$\rho z_w = \mathrm{e}^{-\mathrm{i}k_0 w} \tag{4.3}$$

at every point in the strip, and $\rho(-\mathrm{i}\infty) = (-\mathrm{i}k_0\hat{z}_1)^{-1} \neq 0$. We also introduce a new zero-mean, analytic function, $\nu = \mathrm{i}\rho\Phi_u$. When the kinematic condition is written in the complex form and multiplied by $|\rho|^2$, the choice of ρ and ν becomes transparent, i.e.

$$z_t\bar{z}_u\rho\bar{\rho} - \bar{z}_t z_u \rho\bar{\rho} = \bar{\Phi}_u\rho\bar{\rho} - \Phi_u\rho\bar{\rho}, \tag{4.4}$$

$$\rho z_t \mathrm{e}^{\mathrm{i}k_0 w} - \bar{\rho}\bar{z}_t \mathrm{e}^{-\mathrm{i}k_0 w} = \mathrm{i}(\rho\bar{\nu} + \bar{\rho}\nu), \tag{4.5}$$

where $z_t(w \to -\infty) \to 0$ and the left-hand side is the difference of two complex analytic functions. We apply the projection operator $\hat{P}$ to have

$$\rho z_t \mathrm{e}^{\mathrm{i}k_0 u} = \mathrm{i}\hat{P}[\rho\bar{\nu} + \bar{\rho}\nu]. \tag{4.6}$$

After elementary calculation, we conclude that the new analytic function ρ satisfies the pseudo-differential equation

$$\rho_t = \mathrm{i}(U\rho_u - U_u\rho) - k_0\rho U, \tag{4.7}$$

where U, given by

$$U = \hat{P}(\rho\bar{\nu} + \bar{\rho}\nu), \tag{4.8}$$

is the complex transport velocity. The equation for the complex potential is found by applying $2\hat{P}$ to (3.11):

$$\Phi_t = \mathrm{i}U\Phi_u - B. \tag{4.9}$$

Here B is given by

$$\left.\begin{aligned} B &= \hat{P}\left[\frac{|\Phi_u|^2}{|z_u|^2} - 2\sigma\frac{x_u y_{uu} - y_u x_{uu}}{|z_u|^3}\right], \\ B &= \hat{P}[|v|^2 + 2\sigma k_0|\zeta|^2 + 2\mathrm{i}\sigma(\zeta\bar{\zeta}_u - \bar{\zeta}\zeta_u)], \end{aligned}\right\} \tag{4.10}$$

where $\zeta^2 = \rho$. We omit the trivial details of the calculation and skip to the result, which is the equation satisfied by v:

$$v_t = \mathrm{i}(Uv_u - B_u\rho) - k_0 Uv. \tag{4.11}$$

The newly discovered equation (4.11) is analogous to that originally discovered in Dyachenko (2001) for the infinite fluid domain, and when complemented with (4.7) forms a closed system suitable for numerical simulation.

5. The choice of the reference frame

Equations (4.7) and (4.11) are formulated for the derivative of a conformal map and, henceforth, describe only the motion of the fluid relative to the point of the fluid, $\hat{z}_0$. The motion of this point, namely, $\hat{z}_0(t) = z(-\mathrm{i}\infty)$ is not captured in (4.7) and (4.11) and has to be recovered elsewhere. This missing puzzle piece comes from the momentum conservation that implies the centre of mass of the fluid is an inertial reference frame, and we chose it to be placed at the origin, $z = 0$:

$$\iint_{\mathcal{D}} z\,\mathrm{d}x\,\mathrm{d}y = \iint z|z_u|^2\,\mathrm{d}u\,\mathrm{d}v = 0. \tag{5.1}$$

With the total mass of the fluid being a constant of motion given by

$$m = \iint_{\mathcal{D}} \mathrm{d}x\,\mathrm{d}y, \tag{5.2}$$

(5.1) can be written as

$$m\hat{z}_0 = -\iint (z - \hat{z}_0)|z_u|^2\,\mathrm{d}u\,\mathrm{d}v \tag{5.3}$$

and is used to recover the zero Fourier mode of the conformal map, quite similar to the zero mean condition that is often imposed in the problem with infinite fluid domain. Together with the system (4.7), (4.11) and equation (5.3), we can fully describe the motion of the boundary of the fluid $\partial\mathcal{D}$.

Equations (4.7) and (4.11) for the analytic functions ρ, v are equivalent to the equations for $R = 1/z_u$ and $V = \mathrm{i}\Phi_u R$, i.e.

$$R_t = \mathrm{i}(UR_u - U_u R), \quad V_t = \mathrm{i}(UV_u - B_u R), \tag{5.4a,b}$$

with

$$U = \hat{P}[V\bar{R} + \bar{V}R], \tag{5.5}$$

$$B = \hat{P}[|V^2| + 2\mathrm{i}\sigma(Q\bar{Q}_u - \bar{Q}Q_u)], \tag{5.6}$$

where $Q^2 = R$.

There is, however, an important caveat, namely the function R is no longer analytic at $w \to -\mathrm{i}\infty$, but instead it contains a term in its Fourier series expansion with a positive wavenumber, k_0:

$$R(w) = \mathrm{e}^{\mathrm{i}k_0 w}\left(\hat{\rho}_0 + \sum_{k_0\mathbb{N}} \hat{\rho}_k \mathrm{e}^{-\mathrm{i}kw}\right) = \rho\mathrm{e}^{\mathrm{i}k_0 w}. \tag{5.7}$$

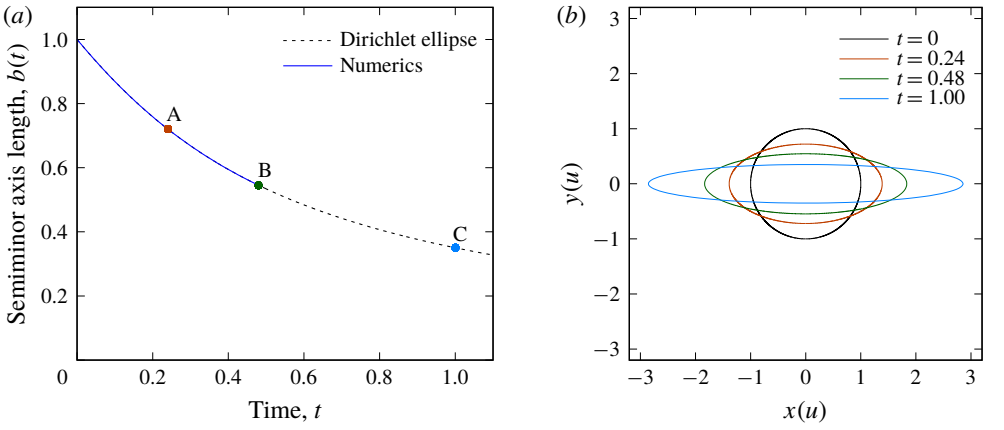

FIGURE 2. (Colour online) (*a*) The size of the semiminor axis of the ellipse according to the theoretical result from Longuet-Higgins (1972) (dashed) and from the direct numerics (solid). The snapshots of the surface shape corresponding to the points labelled by *A*, *B* and *C* are illustrated on the right panel. (*b*) The shape of the fluid boundary at time $t = 0$, $t = 0.24$ (A), $t = 0.48$ (B) and $t = 1.00$ (C). The shape of the surface is found from numerical simulation of (4.7) and (4.11) with initial conditions in accordance with the Dirichlet ellipse (6.5), except for case *C* where the aspect ratio of the ellipse is taken directly from the theory.

6. Numerical experiments

In the remainder of the paper we demonstrate the simulations of (4.7) and (4.11) and compare the results with available exact solutions. The simulations are performed on a uniform grid in the u-variable using the Runge–Kutta fourth-order timestepping scheme. The spatial derivative, ∂_u, and projection operator, $\hat{P}$, are applied as Fourier multipliers to the coefficients of Fourier series of the respective functions.

In the first simulation we compare the solutions of (4.7) and (4.11) with the Dirichlet ellipse (see Longuet-Higgins (1972) for details). The complex potential, Φ, is a quadratic function of the conformal map z for Dirichlet solutions:

$$\Phi = \tfrac{1}{2}Az^2 + \int f \,\mathrm{d}t. \tag{6.1}$$

Here $A = A(t)$ and $\int f \,\mathrm{d}t$ is the Bernoulli constant. The surface shape $\partial\mathcal{D}$ is given by

$$\frac{x^2}{a^2} + \frac{y^2}{b^2} = 1, \tag{6.2}$$

where $a = a(t)$ and $b = b(t)$ are determined from A as follows:

$$a^2 = \frac{1}{b^2} = \frac{A^2}{1 - \sqrt{1 - A^2}} \tag{6.3}$$

and A satisfies an ordinary differential equation (ODE)

$$\frac{\mathrm{d}A}{\mathrm{d}t} = A^2\sqrt{1 - A^4}. \tag{6.4}$$

This ODE is solved numerically and is compared with the solution of (4.7) and (4.11), and agreement is demonstrated in figure 2(*a*). We measure the size of the semiminor

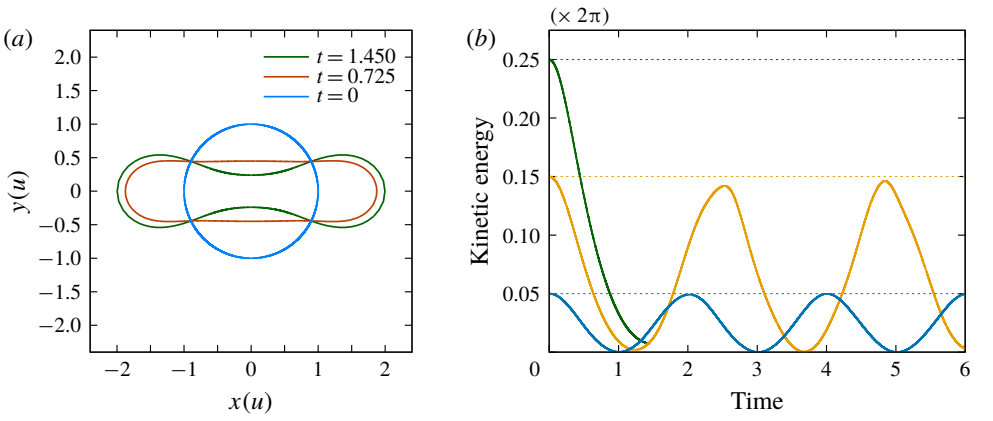

FIGURE 3. (Colour online) Numerical simulation of the motion of a droplet with surface tension coefficient $\sigma = 2$: (*a*) The initial shape of the surface (blue) and the shape of the surface at time $t = 0.725$ (red) and $t = 1.450$ (green) in a simulation with initial kinetic energy $K = 0.25\pi$. The simulation stops when the spectrum of the free surface has become too wide and is not resolved on a uniform grid with 8192 Fourier modes (see figure 4). (*b*) The results of simulations with $c^2 = 0.4$, 1.2 and 2.0 (blue, yellow and green, respectively). The oscillatory motion is exhibited for the blue and yellow curves, but for the green curve (kinetic energy $K = 0.25\pi$) the restoring force from surface tension is insufficient, and the fluid droplet forms a narrowing neck and the droplet breaking is conjectured. We observe that the period of oscillations increases when more kinetic energy is available, and, thus, the restoring force becomes weaker as the droplet extends from its equilibrium shape. Although simulation for $K = 0.25\pi$ stops at time $t = 1.450$, we conjecture that a capillary instability will occur and result in subsequent breaking of the droplet.

axis $b(t)$ as obtained from both simulations and plot the result in figure 2(*b*). The initial data for the simulation is given by

$$\rho(t=0) = 1, \quad v(t=0) = -\sqrt{2}\mathrm{e}^{-\mathrm{i}u}, \tag{6.5a,b}$$

and in the original variables yields

$$z(t=0) = \mathrm{e}^{-\mathrm{i}w}, \quad \Phi(t=0) = \frac{\sqrt{2}}{2}z^2. \tag{6.6a,b}$$

In the second set of simulations, we solve (4.7) and (4.11) in the presence of surface tension with $\sigma = 2$ and take the initial data for the conformal map and the complex potential to be

$$z(t=0) = \mathrm{e}^{-\mathrm{i}w}, \quad \Phi(t=0) = \frac{c}{2}\mathrm{e}^{-2\mathrm{i}w}, \tag{6.7a,b}$$

where the values of c^2 are 0.4, 1.2 and 2.0. At the initial time the surface shape is a unit disc and the complex potential is a quadratic function of z, and if this simulation was run at $\sigma = 0$, then the result would be a Dirichlet ellipse solution. In contrast to the $\sigma = 0$ case, the surface shape exhibits oscillatory motion that is quite similar to standing waves in an infinite fluid, yet surface tension provides the restoring

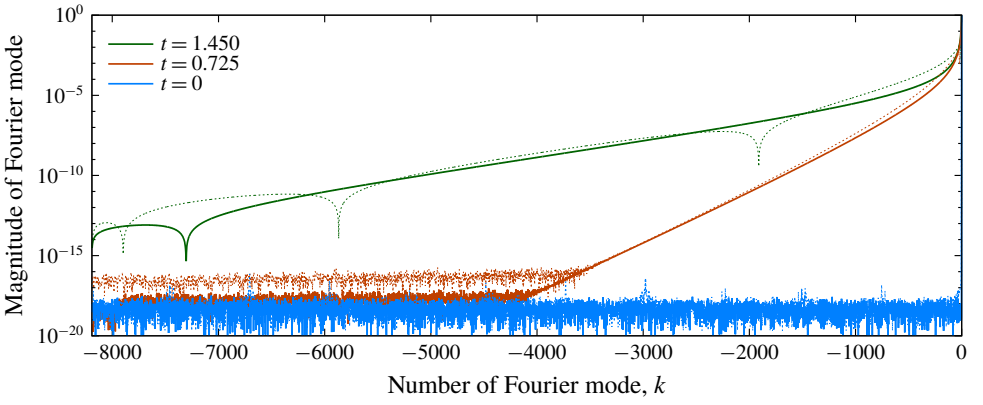

FIGURE 4. (Colour online) Numerical simulation of the motion of a droplet with the surface tension coefficient $\sigma = 2$: the Fourier coefficients $|\hat{\zeta}_k|$ (solid) and $|\hat{\nu}_k|$ (dashed) computed at times $t = 0$ (blue), $t = 0.725$ (red) and $t = 1.425$ (green).

force instead of gravity. In the $c^2 = 2$ case, corresponding to the initial kinetic energy $K = 0.25\pi$, the restoring force is insufficient to lead to droplet oscillations, instead the droplet shape develops a narrowing neck and is reminiscent of fragmentation to smaller droplets (see figure 3).

We measure the accuracy of the simulations by verifying conservation of the fluid mass, m, and the Hamiltonian, $\mathcal{H}$, i.e.

$$\mathcal{H} = -\frac{1}{2}\int \psi \hat{H}\psi_u \,\mathrm{d}u + \sigma \int |z_u| \,\mathrm{d}u, \tag{6.8}$$

which are conserved to 13 digits of precision. In addition, we track the magnitude of Fourier coefficients $|\hat{\zeta}_k|$ and $|\hat{\nu}_k|$ and ensure that it is resolved, illustration of the Fourier spectrum is presented in figure 4.

We observe that given enough kinetic energy the restoring force provided by surface tension becomes incapable of supporting oscillatory motion (see figure 3(*b*)), and it becomes energy efficient to break the droplet into two smaller droplets that carry away half the kinetic energy each, because the characteristic volume of the resulting droplets is halved and the perimeter is decreased by $\sqrt{2}$, the smaller droplets are more stable to further splitting than the initial droplet. However, when the energy is sufficiently large subsequent fragmentation of the smaller droplets may occur.

The actual process of droplet breaking is not tractable with the present techniques of conformal mapping, because at the instant of breaking the topology of the fluid domain changes. Furthermore, as the neck between the two cores extends and its walls close-in, the number of Fourier modes required to resolve the solution grows rapidly, suggesting that singularities in the analytic continuation of ρ and ν are approaching the real axis $v = 0$.

7. Conclusion

A conformal mapping formulation that has been discovered in Dyachenko (2001) for the infinite fluid domain has been extended to a problem of finite, simply connected fluids. The equations describing the free surface are the same as those

in the aforementioned work but with different requirements on analyticity. We have illustrated the extended formulation with the numerical simulations of the Dirichlet ellipse (exact solution), and showed that there is no contradiction to the well-established analytic results for this problem.

We have observed that given sufficiently large initial kinetic energy a droplet may be torn apart. We have demonstrated how a narrow neck is formed in a numerical simulation with surface tension and conjectured that a subsequent capillary instability would result in fragmentation of the droplet. This suggests that multiple breakings to smaller fluid droplets can disperse the energy of a large droplet. It was conjectured that the very same droplet splitting mechanism is at work after a whitecapping event had produced a Crapper-like surface elevation at the crest of a gravity wave, and gives a pathway for a steep ocean wave to shed its energy to a droplet spray.

It is worthwhile to point out that it is typically not recommended to perform simulations on a uniform numerical grid in the u-variable, instead there are techniques to speed-up Fourier series convergence; for details, see Lushnikov, Dyachenko & Silantyev (2017) and Hale & Tee (2009).

The presented work is a precursor to a further study of the droplet splitting problem from the theoretical point of view, and the exact solutions found by Dirichlet, such as the ellipse or the hyperbola, are particularly promising candidates for the droplet splitting via a finite-time singularity formation.

Another subject of ongoing research is the motion of the perturbed boundary of the unit disc in the presence of constant vorticity. The mathematical formulation of this problem is tractable in infinite fluid and the conformal approach is a key ingredient to study the waves with overhanging in infinite domains; see, e.g., Constantin & Strauss (2004) for the travelling wave solutions, and Dyachenko & Mikyoung Hur (2018) for the full time-dependent formulation in the conformal variables. It is perceived that the generalization to the droplet will be tractable as well, and, furthermore, the constant vorticity in a droplet carries more physical meaning than in an infinite depth domain, where it implies unbounded fluid velocities.

Acknowledgements

The author would like to express gratitude to A. Dyachenko, V. M. Hur and F. Pusateri for fruitful discussions. The author thanks the creators and maintainers of the FFTW library Frigo & Johnson (2005) and the entire GNU project. This work was supported by NSF grant DMS-1716822.

REFERENCES

CONSTANTIN, A. & STRAUSS, W. 2004 Exact steady periodic water waves with vorticity. *Commun. Pure Appl. Maths* **57** (4), 481–527.

CONSTANTIN, A., STRAUSS, W. & VĂRVĂRUCĂ, E. 2016 Global bifurcation of steady gravity water waves with critical layers. *Acta Mathematica* **217** (2), 195–262.

CRAPPER, G. D. 1957 An exact solution for progressive capillary waves of arbitrary amplitude. *J. Fluid Mech.* **2**, 532–540.

DA SILVA, A. F. T. & PEREGRINE, D. H. 1988 Steep, steady surface waves on water of finite depth with constant vorticity. *J. Fluid Mech.* **195**, 281–302.

DIRICHLET, G. L. 1860 Untersuchungen über ein Problem der Hydrodynamik. *Abh. Kön. Gest. Wiss. Göttingen* **8**, 3–42.

DYACHENKO, A. I. 2001 On the dynamics of an ideal fluid with a free surface. *Dokl. Math.* **63**, 115–117.

DYACHENKO, A. I., KUZNETSOV, E. A., SPECTOR, M. D. & ZAKHAROV, V. E. 1996*a* Analytical description of the free surface dynamics of an ideal fluid (canonical formalism and conformal mapping). *Phys. Lett.* A **221** (1), 73–79.

DYACHENKO, A. I., ZAKHAROV, V. E. & KUZNETSOV, E. A. 1996*b* Nonlinear dynamics of the free surface of an ideal fluid. *Plasma Phys. Rep.* **22** (10), 829–840.

DYACHENKO, S. & NEWELL, A. C. 2016 Whitecapping. *Stud. Appl. Maths* **137** (2), 199–213.

DYACHENKO, S. A. & MIKYOUNG HUR, V. 2018 Stokes waves with constant vorticity. Part I. Numerical computation. Preprint, arXiv:1802.07671.

FRIGO, M. & JOHNSON, S. G. 2005 The design and implementation of fftw3. *Proc. IEEE* **93** (2), 216–231.

HALE, N. & TEE, T. W. 2009 Conformal maps to multiply slit domains and applications. *SIAM J. Sci. Comput.* **31** (4), 3195–3215.

LONGUET-HIGGINS, M. S. 1972 A class of exact, time-dependent, free-surface flows. *J. Fluid Mech.* **55** (3), 529–543.

LUSHNIKOV, P. M., DYACHENKO, S. A. & SILANTYEV, D. A. 2017 New conformal mapping for adaptive resolving of the complex singularities of Stokes wave. *Proc. R. Soc. Lond.* A **473**, 20170198.

RIBEIRO, R., MILEWSKI, P. A. & NACHBIN, A. 2017 Flow structure beneath rotational water waves with stagnation points. *J. Fluid Mech.* **812**, 792–814.

RUBAN, V. P. 2004 Water waves over a strongly undulating bottom. *Phys. Rev.* E **70**, 066302.

STOKES, G. G. 1880 *Mathematical and Physical Papers*, vol. 1. Cambridge University Press.

TANVEER, S. 1993 Singularities in the classical rayleigh-taylor flow: formation and subsequent motion. *Proc. R. Soc. Lond.* A **441** (1913), 501–525.

TITCHMARSH, E. C. 1986 *Introduction to the Theory of Fourier Integrals*, 3rd edn. Chelsea Publishing Co.

TURITSYN, K. S., LAI, L. & ZHANG, W. W. 2009 Asymmetric disconnection of an underwater air bubble: Persistent neck vibrations evolve into a smooth contact. *Phys. Rev. Lett.* **103**, 124501.

ZAKHAROV, V. E. 1968 Stability of periodic waves of finite amplitude on the surface of a deep fluid. *J. Appl. Mech. Tech. Phys.* **9** (2), 190–194.

ZAKHAROV, V. E., DYACHENKO, A. I. & VASILYEV, O. A. 2002 New method for numerical simulation of a nonstationary potential flow of incompressible fluid with a free surface. *Eur. J. Mech. (*B*/Fluids)* **21** (3), 283–291.